Multiferroic phase competitions in perovskite manganite thin films

M. H. Qin, Y. M. Tao, M. Zeng, X. S. Gao, S. J. Wu et al.

Citation: Appl. Phys. Lett. **100**, 052410 (2012); doi: 10.1063/1.3682079
View online: http://dx.doi.org/10.1063/1.3682079
View Table of Contents: http://apl.aip.org/resource/1/APPLAB/v100/i5
Published by the American Institute of Physics.

Multiferroic phase competitions in perovskite manganite thin films

M. H. Qin,[1] Y. M. Tao,[2] M. Zeng,[1] X. S. Gao,[1] S. J. Wu,[1] S. Dong,[3] and J.-M. Liu[2,4,a)]
[1]*Institute of Advanced Materials, School of Physics, South China Normal University, Guangzhou 510006, China*
[2]*Laboratory of Solid State Microstructures, Nanjing University, Nanjing 210093, China*
[3]*Department of Physics, Southeast University, Nanjing 211189, China*
[4]*International Center for Materials Physics, Chinese Academy of Science, Shenyang 110016, China*

(Received 13 September 2011; accepted 15 January 2012; published online 3 February 2012)

Based on the Mochizuki-Furukawa model, the cycloidal spin structures of orthorhombic $R\mathrm{MnO_3}$ manganite thin films on various magnetic substrates are simulated using Monte Carlo method. It is revealed that the long range cycloidal spin order can be modulated by the film thickness and substrate spin structure. In particular, the ferromagnetic and antiferromagnetic spin orders of the substrate in different orientations have different pinning effects on the cycloidal spin order of the thin film. The simulated results are discussed in terms of the competition between the single-ion anisotropy and spin-orbit coupling. © *2012 American Institute of Physics*. [doi:10.1063/1.3682079]

Multiferroicity is attracting continuous attentions due to the interesting physics and potential applications.[1–4] Especially, type-II multiferroics, such as cycloidal magnets, orthorhombic manganites $R\mathrm{MnO_3}$ (R = Tb, Dy, $\mathrm{Eu_{1-x}Y_x}$, etc.),[5–7] $\mathrm{Ni_3V_2O_8}$,[8] and $\mathrm{MnWO_4}$,[9] have been addressed due to the unusual fact that the ferroelectricity is generated by frustrated spin orders. The spin current theory and the inverse Dzyaloshinskii-Moriya (DM) interaction model were proposed in order to understand the underlying microscopic mechanism.[10–12] It is believed that the spin-orbit coupling for two adjacent spins S_i and S_j separated by vector r_{ij} can generate a local polarization $P_{ij} \propto -r_{ij} \times (S_i \times S_j)$. Thus, a macroscopic ferroelectric (FE) polarization P can be induced because spin-helicity vector h defined as $S_i \times S_j$ is associated with a ferroic alignment. Taking orthorhombic manganites $R\mathrm{MnO_3}$ as examples, polarization P along the a-axis is induced in the ab-plane cycloidal spin (ab-CS) phase with propagation vector Q along the b-axis, while it is induced along the c-axis in the bc-plane cycloidal spin (bc-CS) phase, as illustrated in Figs. 1(a) and 1(b). In addition, several theoretical works on the origin for the CS order and magnetoelectric (ME) coupling in $R\mathrm{MnO_3}$ are available.[13,14]

Recently, Mochizuki and Furukawa proposed a classical Heisenberg spin model (M-F model) which includes the superexchange interaction, the single-ion anisotropy (SIA), the DM interaction, and the cubic anisotropy, to study the phase diagrams of $R\mathrm{MnO_3}$.[14] The ab-CS state is stabilized by the SIA and the DM interaction with vectors on the in-plane Mn-O-Mn bonds, while the bc-CS state is stabilized by the DM interaction with vectors on the out-of-plane Mn-O-Mn bonds. The R-site ionic radius mainly controls the lattice distortion which tunes the SIA and the DM interaction, thus in turn determines the competition between the ab-CS phase and bc-CS phase. This leads to the flop of the cycloidal plane from the ab-plane to the bc-plane with decreasing R-ion radius. It has been demonstrated that this model can explain the complicated multiferroic behaviors.[15–20]

While the physics of multiferroics is being progressively understood, researches proceed in related device designs where multiferroic thin films are expected to play an important role.[21,22] Understanding of the phase competitions in multiferroic thin films certainly becomes interested not only from the point of view of the physics responsible for multiferroic spin orders in this specific geometry, but more for insight in the design of advanced devices. However, so far rare work along this line is available and one of the main issues is that measurement of polarization in those type-II multiferroic thin films remains unsuccessful, while relevant theoretical progress is under the way. In this work, we address the multiferroic behaviors of a model orthorhombic $R\mathrm{MnO_3}$ thin film deposited epitaxially on a substrate by theoretical simulation. For simplicity, we focus on the impact of

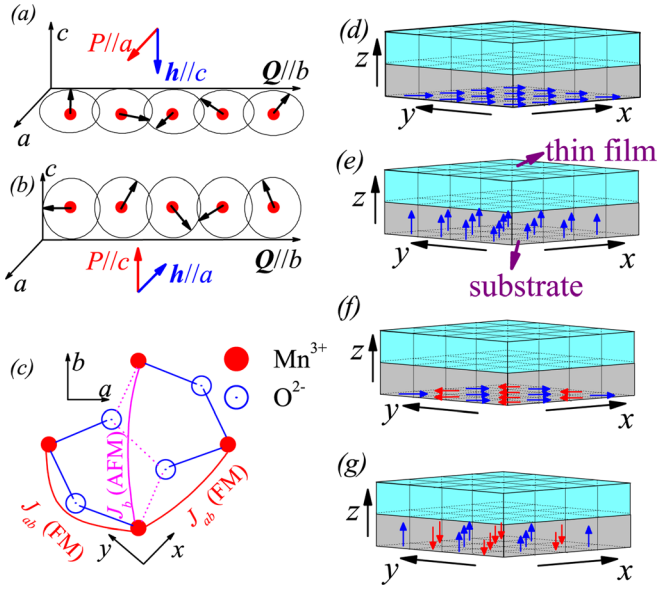

FIG. 1. (Color online) Induced electric polarization P and spin-helicity vector $h = \Sigma_{i/S_i} \times S_j$ in (a) the ab-CS and (b) bc-CS states. (c) Crystal structure (ab-plane) of orthorhombically distorted $R\mathrm{MnO_3}$. Sketch of thin film (top turquoise layer) grown on the magnetic substrate (bottom grey layer) in which all spins are fixed to the FM pattern with (d) $S_s//a$ and (e) $S_s//c$, and to the AFM pattern with (f) $S_s//a$ and (g) $S_s//c$.

a)Author to whom correspondence should be addressed. Electronic mail: liujm@nju.edu.cn.

thin film thickness and substrate magnetic structure, while the lattice mismatch between the substrate and thin films is ignored at this stage. For the magnetic structure of the substrate, we limit our discussion on three types of substrates: (1) without magnetism, (2) of simple ferromagnetic (FM) order, and (3) of antiferromagnetic (AFM) order. In the latter two cases, the spin alignments of the substrate along various orientations (spin moment $S_s = 2$) are fixed as shown in Figs. 1(d)–1(g), implying that the spin interaction in the substrate is no exception much stronger than that in the thin film so that the bottom layer of the thin film is pinned off.

In our simulation, the M-F model with Mn spin $S = 2$ on a cuboidal lattice is used.[14] The Hamiltonian can be written as $H = H_{ex} + H_{sia} + H_{DM} + H_{cub}$. The first term $H_{ex} = \Sigma_{\langle ij \rangle} J_{ij} \cdot (S_i \cdot S_j)$ is the spin exchange interactions with $J_{ab} = -0.8$ and $J_b = 0.8$ the coupling constants in the Mn-Mn bonds on the *ab*-plane (Fig. 1(c)), $J_c = 1.25$ the AFM exchange in the bonds along the *c*-(z-) axis. Here, the energy unit is meV. The second term is the SIA term $H_{sia} = D \cdot \Sigma_i S^i_{\zeta i} + E \cdot \Sigma_i (-1)^{ix+iy} \cdot (S^i_{\xi i} - S^i_{\eta i})$ with $D = 0.25$, $E = 0.30$, here, ξ_i, η_i, ζ_i are the tilted local axes attached to the *i*-th MnO_6 octahedron.[14] For their direction vectors, we use experimental data of $EuMnO_3$ for simplicity.[23] The third term H_{DM} denotes the DM interactions $H_{DM} = \Sigma_{\langle ij \rangle} d_{i,j} \cdot (S_i \times S_j)$, where factors $d_{i,j}$ are determined by five DM parameters, $(\alpha_{ab}, \beta_{ab}, \gamma_{ab}) = (0.10, 0.10, 0.14)$ and $(\alpha_c, \beta_c) = (0.30, 0.30)$. The last term $H_{cub} = A \cdot \Sigma_i (S^4_{xi} + S^4_{yi} + S^4_{zi})/S(S+1)$ represents the cubic anisotropy with coupling constant $A = 0.0162$.

The thin film is considered to be a three-dimensional (3D) half-infinite cuboidal lattice, e.g., infinite in the *x* and *y* directions, but finite in the *z* direction. The periodic boundary conditions are applied in the *x*- and *y*-axis directions, and the free boundary condition is applied onto the top layer along the *z* direction. The spins in the bottom layer are coupled with the spins of the substrate. Our simulation is performed on a $36 \times 36 \times L_z$ (unless stated elsewhere, $L_z = 6$ is chosen, and in fact the results for $L_z > 6$ show no much difference) cuboidal lattice using standard Metropolis algorithm and temperature exchange method.[24,25] Specific heat $C(T) = (\langle H^2 \rangle - \langle H \rangle^2)/Nk_BT^2$ and spin-helicity vector $h_\gamma(T) = \langle |\Sigma_i S_i \times S_{i+b}| \rangle / NS^2$ ($\gamma = a, b, c$) as a function of temperature (T) are calculated to determine the transition points and spin structure, here N is the number of Mn ions, k_B is the Boltzmann constant, and the brackets denote thermal and configuration averaging. It is expected that $h_c(h_a)$ has a large value for the *ab*-CS (*bc*-CS) order, while all of these three components of h_γ should be zero in the paramagnetic (PM) phase and sinusoidal collinear antiferromagnetic (sc-AFM) phase.

As a comparison, Fig. 2(a) shows the simulated $C(T)$ and $h_\gamma(T)$ for bulk case. The $C(T)$ curve shows three peaks, indicating successive three phase transitions with decreasing T. The first one is the transition from the PM phase to the sc-AFM phase at T_N. At the second transition point T_{bc}, $h_a(T)$ increases, indicating a transition of the sc-AFM phase to the *bc*-CS phase. When T falls down to the third transition point T_{ab}, $h_a(T)$ suddenly drops, accompanied with a steep increase of $h_c(T)$, indicating a transition from the *bc*-CS order to the *ab*-CS order.

Looking at the simulated data for the thin film on a non-magnetic substrate ($S_s = 0$) allows an investigation of the

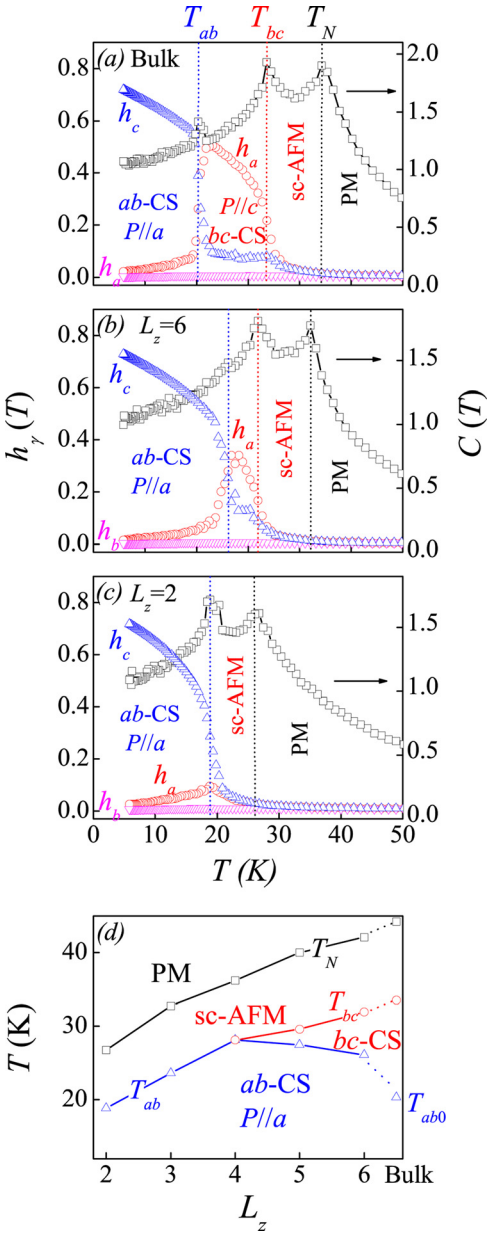

FIG. 2. (Color online) Specific heat $C(T)$ and spin-helicity vector $h_\gamma(T)$ ($\gamma = a, b, c$) as a function of T in (a) the bulk system, and in thin films with (b) $L_z = 6$, (c) $L_z = 2$. (d) The phase diagram in the (L_z, T) plane.

effect of the thin film thickness. The simulated results with $L_z = 6$ are shown in Fig. 2(b). Point T_N is slightly lower than that for the bulk case. What is interested is the enhanced T_{ab}, implying that the *bc*-CS order is suppressed in compensation with the promoted stability of the *ab*-CS order. This tendency continues upon further decreasing of L_z till the *bc*-CS phase is completely suppressed, leaving the *ab*-CS phase at low T side.

The disappearance of the *bc*-CS phase with decreasing thin film thickness is easily understood at the first glance. The DM interaction with vectors on the out-of-plane Mn-O-Mn bonds stabilizes the *bc*-CS order. In case of no DM interaction, the angles between the nearest two spins along the *c*-axis are $\phi_c = \pi$, due to the strong AFM coupling J_c. Inclusion of the DM interaction allows the angles to be alternatively modulated as $(\pi - \Delta\phi_c)$ and $(\pi + \Delta\phi_c)$ with $\Delta\phi_c > 0$. The energy gain from the DM interaction, due to

this modulation, is $\Delta E_{DM}/N = -\alpha_c S^2 |\cos\phi_c| \Delta\phi_c = -\alpha_c S^2 \Delta\phi_c$ with α_c the magnitude of the a-component of the DM vectors on the out-of-plane bonds. This energy gain is reduced with the film thickness since the spins on the up and bottom layers lack of this contribution, leading to the destabilization of the bc-CS phase.

On the other hand, the ab-CS order which is mainly stabilized by the SIA, less relevant with the DM interaction with vectors on the in-plane Mn-O-Mn bonds. As a result, the ab-CS phase is enhanced in energy with respect to the bc-CS phase. Both T_N and T_{bc} shift seriously downward with decreasing film thickness and as an extreme case with $L_z = 2$, shown in Fig. 2(c), T_{bc} disappears, leaving only the ab-CS phase at low-T side. What should be mentioned is that upon decreasing film thickness, T_{ab} first increases from the value (T_{ab0}) for the bulk case, and then decreases down to T_{ab0} at $L_z = 2$. This indicates that the sc-AFM order and bc-CS order are strongly suppressed, while the ab-CS order at low T remains quite robust. Because the ab-CS order is mainly determined by the ab-plane spin interaction, the present results are easily understood.

As a summary, we present the simulated phase diagram in the (L_z, T) plane of the spin structure in Fig. 2(d), from which the remarkable film-thickness dependence of the spin structure including the ferroelectric CS order is clearly shown. In fact, similar phenomenon was observed in earlier work in which the spiral spin structure in bulk $TbMnO_3$ can be intensively suppressed in epitaxially strained thin film form.[26]

Subsequently, one comes to look at the impact of the spin structure from the substrate. For a FM substrate with the spins aligning along either the a-axis or c-axis (in-plane or out-of-plane), Figs. 3(a) and 3(b) show the simulated results. It is clearly shown that the ab-CS order and bc-CS order are suppressed completely respectively for the in-plane and out-of-plane cases, while the sc-AFM order remains nearly unaffected.

To some extent, the effect of the FM substrate with $S_s//a$ ($S_s//c$) is similar to that of the applied magnetic filed $B//a$ ($B//c$) onto the bottom layer because of the strong AFM coupling J_c. Meanwhile, B tends to align the spins in perpendicular to B for a cycloidal spin system. As a result, the bc-CS (ab-CS) order is stabilized in the bottom layer, and in turn be extended to the whole film system to satisfy the energy relation for the case of the FM substrate with $S_s//a$ ($S_s//c$). In addition, it is noted that T_N for the two cases are almost identical, indicating that the transition from the PM phase to the sc-AFM order is mainly determined by the lattice size of the film.

At last, the effect of the AFM substrate on multiferroic properties is studied. It is indicated that the ab-CS order is enhanced for the case of the AFM substrate with $S_s//a$, as shown in Fig. 3(c). Being different from the FM substrate, the AFM one with $S_s//a$ tends to align the spins of the bottom layer in the ab-plane to satisfy the AFM coupling J_c. At the same time, the DM interaction with vectors on the in-plane bonds and the SIA stabilize the ab-CS order. This leads to the flop of the cycloidal plane from the bc-plane to the ab-plane. On the other hand, the AFM substrate with $S_s//c$ may enlarge the T region with the bc-CS order. This argument has been proved in our simulated results, as shown in Fig. 3(d). The transition from the bc-CS order to the ab-CS order in the pinning system occurs at a much lower T than that in non-pinning system (Fig. 2(b)), demonstrating that the ab-CS order is extensively suppressed for this case.

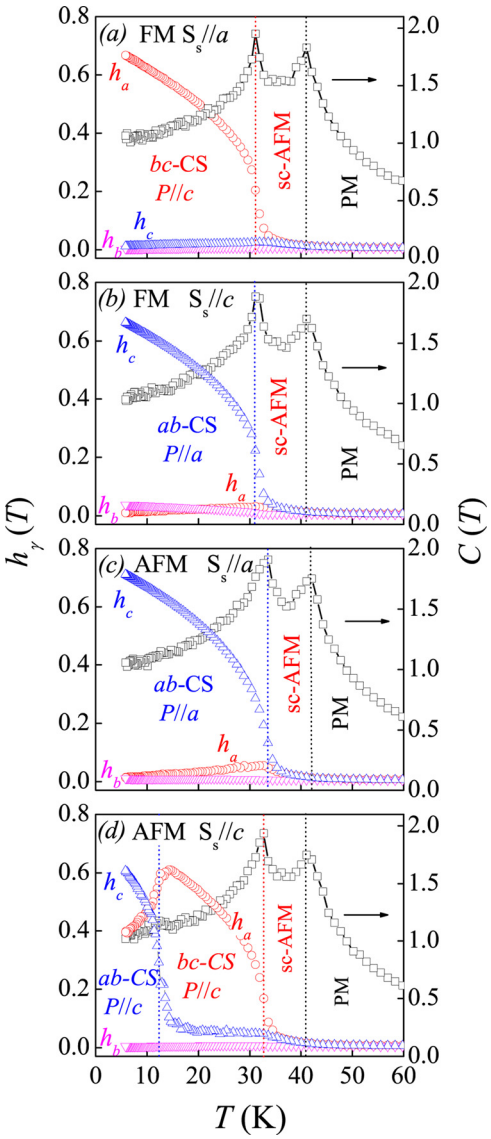

FIG. 3. (Color online) Specific heat $C(T)$ and spin-helicity vector $h_\gamma(T)$ ($\gamma = a, b, c$) as a function of T in thin film grown on the FM pinning substrate (a) with $S_s//a$, and (b) with $S_s//c$, and the AFM pinning substrate (a) with $S_s//a$, and (b) with $S_s//c$.

Up to now, there is an urgent need in studying multiferroic film to develop a better understanding of the evolution of ME properties in the special geometries. In this work, the multiferroic properties in orthorhombic manganites film are studied based on the M-F model. It is demonstrated that the long range cycloidal orders can be significantly modulated by the film thickness and substrate spin structure. In addition, our simulation indicates that the magnetic substrate may have a significantly pinning effect on the multiferroic behaviors in film systems. The simulated results are discussed from the energy landscape in details. Our simulation is helpful to understand the phase competitions, and provides useful information for practical applications of $RMnO_3$ film. Of course, the prediction given here deserves to be checked in further experiments.

This work was supported by the Natural Science Foundation of China (50832002, 51072061, and 51031004), the National Key Projects for Basic Researches of China (2009CB623303 and 2009CB929501), the China Postdoctoral Science Foundation (20100480768), and the Priority Academic Program Development of Jiangsu Higher Education Institutions, China.

[1]M. Fiebig, J. Phys. D **38**, R123 (2005).
[2]W. Eerenstein, N. D. Mathur, and J. F. Scott, Nature **442**, 759 (2006).
[3]S.-W. Cheong and M. Mostovoy, Nature Mater. **6**, 13 (2007).
[4]K. F. Wang, J.-M. Liu, and Z. F. Ren, Adv. Phys. **58**, 321 (2009).
[5]T. Kimura, T. Goto, H. Shintani, K. Ishizaka, T. Arima, and Y. Tokura, Nature **426**, 55 (2003).
[6]T. Goto, T. Kimura, G. Lawes, A. P. Ramirez, and Y. Tokura, Phys. Rev. Lett. **92**, 257201 (2004).
[7]J. Hemberger, F. Schrettle, A. Pimenov, P. Lunkenheimer, V. Y. Ivanov, A. A. Mukhin, A. M. Balbashov, and A. Loidl, Phys. Rev. B **75**, 035118 (2007).
[8]G. Lawes, A. B. Harris, T. Kimura, N. Rogado, R. J. Cava, A. Aharony, O. Entin-Wohlman, T. Yildirim, M. Kenzelmann, C. Broholm *et al*., Phys. Rev. Lett. **95**, 087205 (2005).
[9]K. Taniguchi, N. Abe, T. Takenobu, Y. Iwasa, and T. Arima, Phys. Rev. Lett. **97**, 097203 (2006).
[10]H. Katsura, N. Nagaosa, and A. V. Balatsky, Phys. Rev. Lett. **95**, 057205 (2005).
[11]M. Mostovoy, Phys. Rev. Lett. **96**, 067601 (2006).
[12]I. A. Sergienko and E. Dagotto, Phys. Rev. B **73**, 094434 (2006).
[13]S. Dong, R. Yu, S. Yunoki, J.-M. Liu, and E. Dagotto, Phys. Rev. B **78**, 155121 (2008).
[14]M. Mochizuki and N. Furukawa, Phys. Rev. B **80**, 134416 (2009).
[15]M. Mochizuki and N. Furukawa, Phys. Rev. Lett. **105**, 187601 (2010).
[16]M. Mochizuki, N. Furukawa, and N. Nagaosa, Phys. Rev. Lett. **104**, 177206 (2010).
[17]M. Mochizuki and N. Nagaosa, Phys. Rev. Lett. **105**, 147202 (2010).
[18]M. Mochizuki, N. Furukawa, and N. Nagaosa, Phys. Rev. Lett. **105**, 037205 (2010).
[19]M. H. Qin, Y. M. Tao, S. Dong, H. B. Zhao, X. S. Gao, and J.-M. Liu, Appl. Phys. Lett. **98**, 102510 (2011).
[20]Y. M. Tao, M. H. Qin, S. Dong, X. S. Gao, and J.-M. Liu, J. Appl. Phys. **109**, 113909 (2011).
[21]G. Lawes and G. Srinivasan, J. Phys. D: Appl. Phys. **44**, 243001 (2011).
[22]L. W. Martin, Y. H. Chu, and R. Ramesh, Mater. Sci. Eng. R **68**, 89 (2010).
[23]B. Dabrowski, S. Kolensnik, A. Baszczuk, O. Chmaissem, T. Maxwell, and J. Mais, J. Solid State Chem. **178**, 629 (2005).
[24]D. P. Landau and K. Binder, *A Guide to Monte Carlo Simulations in Statistical Physics* (Cambridge University Press, Cambridge, England, 2005).
[25]K. Hukushima and K. Nemoto, J. Phys. Soc. Jpn. **65**, 1604 (1996).
[26]C. J. M. Daumont, D. Mannix, S. Venkatesan, G. Catalan, D. Rubi, B. J. Kooi, J. Th. M. De Hosson, and B. Noheda, J. Phys.: Condens. Matter **21**, 182001 (2009).